

Simulated Rarefied Aerodynamics of the Magellan Spacecraft During Aerobraking

Brian L. Haas*

Thermosciences Institute, Moffett Field, California 94035-1000

and

Durwin A. Schmitt†

Martin Marietta Astronautics Company, Denver, Colorado 80233

Aerodynamic loads upon the Magellan spacecraft during aerobraking through the atmosphere of Venus are computed at off-design attitudes with a direct simulation Monte Carlo (DSMC) particle method. This method is not restricted to the assumption of collisionless flow normally employed to assess spacecraft aerodynamics. Simulated rarefied flows at nominal altitudes near 140 km and an entry speed of 8.6 km/s were compared with simulated and analytic free-molecular results. Aerodynamic moments, forces, and heating for rarefied entry at all attitudes were 7–10% below free-molecular results. All moments acted to restore the vehicle to its nominal zero-pitch, zero-yaw attitude. Suggested canting of the solar panels is an innovative configuration to assess gas-surface interaction during aerobraking. The resulting roll torques about the central body axis, as predicted in rarefied-flow simulations, were nearly twice that predicted for free-molecular flow, although differences became less distinct for thermal accommodation coefficients well below unity. In general, roll torques increased dramatically with reduced accommodation coefficients employed in the simulation. In the DSMC code, periodic free-molecule boundary conditions and a coarse computational grid and body resolution served to minimize the simulation size and cost while retaining solution validity.

Nomenclature

A_f	= vehicle frontal area (236.8 cell ²)
a	= thermal accommodation coefficient
D	= diameter of the HGA (370 cm, 11.77 cells)
F	= aerodynamic force coefficient
Kn	= Knudsen number, λ/D
M	= Mach number or moment coefficient
m	= molar mass of atmospheric gas
n	= number density
Q	= incident freestream energy flux, $\rho_\infty u_\infty^3/2$
q	= net heat flux on solar panels
T	= temperature
u	= flow velocity
x axis	= roll axis, along central body axis
y axis	= yaw axis, through solar-panel axes
z axis	= pitch axis
α	= intermolecular potential exponent
ϵ	= surface radiative emissivity
λ	= gas mean free path
ρ	= gas mass density, kg/m ³

Subscript

∞ = value at freestream conditions

Introduction

The Magellan spacecraft began mapping the surface of Venus from a highly elliptic orbit (eccentricity $e = 0.39$) in September of

1990. Mission planners at NASA's Jet Propulsion Laboratory (JPL) then wished to circularize the orbit to improve mapping, but could not perform the maneuver through thruster activity alone because of limited remaining propellant. The orbital maneuver was achieved instead through a series of gentle passes through the Venus atmosphere (approximately 840 passes with an average velocity decrement of 1.5 m/s each)¹ from late May through early August of 1993. Besides nearly circularizing the orbit, these maneuvers provided some limited data related to atmospheric entry of satellite spacecraft.

The spacecraft configuration is depicted in Fig. 1 in its nominal entry orientation (three-axis stabilized) with flow directed along the central body axis (x axis) such that the high gain antenna is aft. The solar panels in this configuration are normal to the flow, but may be canted at any angle (about the y axis) to form an effective "windmill" during entry. The restoring roll torques on the spacecraft may be measured, along with surface heating and orbit altitudes, to deduce the flowfield density and the surface accommodation coefficients in the normal and tangential directions. Axes for pitch and yaw are indicated in the front view.

One critical mission constraint is the aerodynamic heating on the delicate solar panels during each aeropass. Direct particle simulations of entry at several altitudes from 125 to 140 km in the nominal orientation² verified that this heating was within the specified tolerance, at altitudes exceeding 135 km, under the conservative assumption of full gas-surface thermal accommodation. At the nominal altitude of 140 km, the heating and drag results corresponding to the rarefied flow were very close to those corresponding to free-molecular (collisionless) flow at that altitude.

Prior to aerobraking, mission planners were also concerned with spacecraft stability during the maneuvers, particularly if the entry orientation had a high angle of pitch or yaw. To address such concerns, simplified aerodynamic analyses rely upon the assumption of free-molecular flow and may be computed reliably with the FREEMAC code.³ However, this assumption may not be valid at nominal flight conditions when the freestream Knudsen number is below 10 [based upon the high-gain antennae (HGA) diameter]. The objective of the present study was to calculate torques, forces, and heating of the Magellan spacecraft for several entry attitudes, employing a Direct simulation Monte Carlo particle method that is not restricted to the assumption of free-molecular flow. The results of the rarefied simulation were then compared with FREEMAC results

Presented as Paper 93-3676 at the AIAA Atmospheric Flight Mechanics Conference, Monterey, CA, Aug. 9–11, 1993; received Aug. 17, 1993; revision received March 11, 1994; accepted for publication March 14, 1994. Copyright © 1994 by the American Institute of Aeronautics and Astronautics, Inc. No copyright is asserted in the United States under Title 17, U.S. Code. The U.S. Government has a royalty-free license to exercise all rights under the copyright claimed herein for Governmental purposes. All other rights are reserved by the copyright owner.

*Research Scientist, M/S 230-2 NASA Ames Research Center. Member AIAA.

†Retired; currently Vice President, Tactical Technical Solutions, P.O. Box 656, Broomfield, CO 80038.

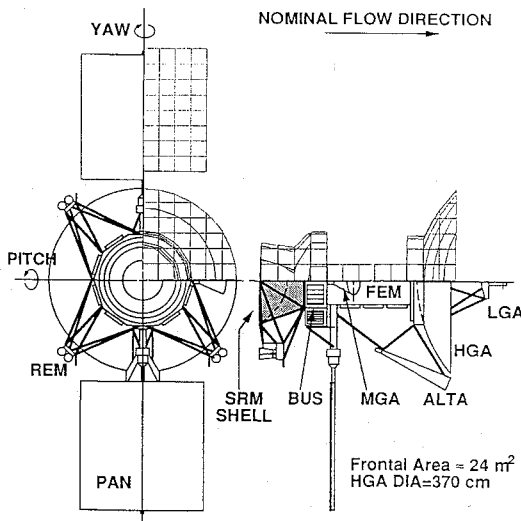


Fig. 1 Magellan spacecraft configuration and simulated geometry at nominal zero pitch and yaw.

to assess the significance of molecular collisions in the flow. A similar study by Rault⁴ employed a DSMC method and a very fine body resolution. However, some of Rault's free-molecule results were questionable, since they differed significantly from FREEMAC results, perhaps as a result of inconsistent moment reference locations.

Roll torques associated with the windmill entry configurations were also computed in the present work at nominal conditions and compared with free-molecule results. Aerodynamic sensitivity to the assumed surface thermal accommodation coefficient was assessed for the windmill configuration. The nominal altitudes were 136–140 km, and the periapsis velocity was $u_\infty = 8.6$ km/s.

Particle Simulation Method

Direct simulation Monte Carlo (DSMC) particle methods model the motion and interaction of thousands or millions of computational particles to simulate gasdynamics.⁵ Specifics of the DSMC code employed in these studies are provided in Ref. 2. Given a particular position, velocity, and internal energy status, each particle in the flowfield travels unobstructed along the linear trajectory of its velocity vector over the duration of a single time step. Neighboring particles are then identified throughout the flowfield and paired off as potential collision candidates. The flowfield is divided into a network of uniform cubic cells to facilitate identification of neighboring particles and to define the finest resolution for sampling macroscopic flow properties. Employing probabilities as functions of individual collision parameters such as collision cross section and relative translational speed,⁶ the subset of all candidate pairs that collide during the time step are identified. In simulating free-molecule flow, the probability of collision is artificially set to zero, representing an infinite molecular mean free path.

The entire simulated flowfield is initialized with freestream conditions. The particle simulation then runs through a transient phase as the solution develops and flowfield structures form. Upon reaching steady state, the simulation collects statistical samples for measuring properties of the flowfield and body surface fluxes.

The DSMC code employed in the present study was developed by McDonald⁷ for efficient implementation on vector supercomputers. This code simulates nonreactive three-dimensional flow of general gas mixtures about arbitrary geometries. Molecular collisions pertain to the variable-hard-sphere model of Bird^{6,8} with an inverse intermolecular potential exponent $\alpha = 5$ to simulate the gas dominated by CO₂. As discussed in detail in Ref. 2, the internal energy modes are modeled with three fully excited degrees of freedom to take account of molecular rotation and vibration. Internal energy excitation is performed with the mechanics of Borgnakke and Larsen,⁹ employing a fixed probability of relaxation of one-fifth.

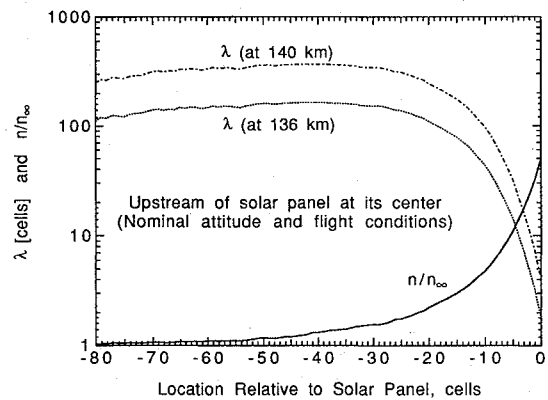


Fig. 2 Stagnation streamline profiles of number density and molecular mean free path.

Body Geometry and Grid

The geometry of the Magellan spacecraft is shown in Fig. 1 and compared with the simulated geometry. Because of the large mean free path in the flow about the spacecraft, small features on the vehicle such as the altimeter antenna (ALTA), the medium- and low-gain antennas (MGA, LGA), and the rocket engine modules (REM) have negligible effect on the flowfield as a whole and may be excluded to simplify the simulation geometry, leading to two planes of symmetry on the vehicle. These small features do affect the vehicle aerodynamics, however, and their contribution will be considered separately.

To represent a surface in the cubic Cartesian grid network of the simulation, it is necessary to approximate the surface as a composite of planar facets. Each facet has a normal defined from the intersections of the surface with the edges of the cell. This faceted description of the body is appropriate given that body radii are large in comparison with the cell size, and that the intersection of different surfaces occurs at cell boundaries. Since the solar panels and HGA are dominant components of the structure, the simulation cell network was scaled so that the square simulated panels (measuring 8×8 cells) have the same frontal area as the actual solar panels and that the HGA diameter (11.77 cells) matches the actual HGA via scaling factor, 1 cell = 31.44 cm. Such a coarse grid and body resolution was used in this study to reduce the computational expense associated with running several simulations.

Grid resolution greatly affects the accuracy of DSMC solutions for vehicle aerodynamics and heating in rarefied flows. An established criterion for sufficient grid resolution is that the local mean free path must exceed the cell dimension. For cold-wall blunt-body rarefied flows, the flowfield density will likely be quite large near the body surface, leading to a small stagnation mean free path. "Cold-wall" implies that the surface temperature is of the order of T_∞ while being significantly below the peak flow temperature upstream of the body. Equilibrium kinetic theory provides the following simple estimate of the local mean free path¹⁰ near the body surface,

$$\frac{\lambda}{\lambda_\infty} \approx \frac{n_\infty}{n} \left(\frac{T}{T_\infty} \right)^{2/\alpha} \quad (1)$$

Simulated at nominal flight conditions, the flow density n , local mean free path λ , and temperature T along the stagnation streamline at the center of the solar panel are plotted in Figs. 2 and 3. Here, T is defined in the rarefied simulation by the variance of the molecular velocity distribution of the particles. Flow properties at the panel surface led to stagnation mean free paths in the range $1.8 < \lambda < 4.2$ cells, exceeding the minimum accuracy criterion at all altitudes.

Body surfaces are modeled^{11,12} as if in radiative equilibrium with deep space at a temperature of 4 K and with an emissivity $\epsilon = 0.82$. Advantages of this model include: 1) it is simple to implement in the simulation; 2) it does not require a prescribed estimate of the surface temperature; and 3) it allows each surface facet to reach its own temperature independent of neighboring facets. It is assumed that radiation from the flowfield or from other body surfaces would contribute negligibly to the net heating of a given surface facet. Most results will employ a thermal accommodation coefficient of unity,

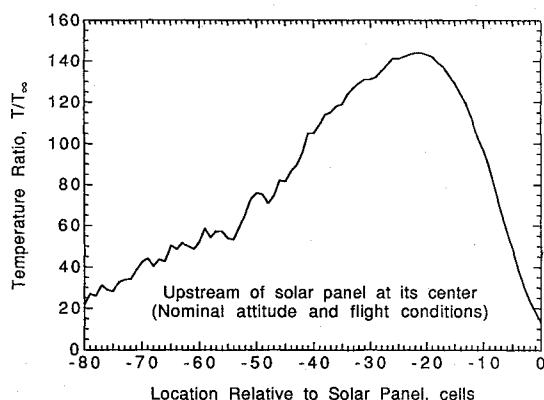


Fig. 3 Stagnation streamline temperature profile.

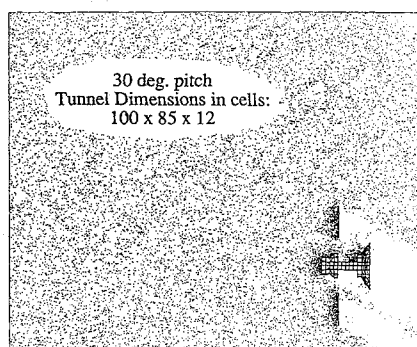


Fig. 4 Simulation geometry and flow domain.

typical of rough cool surfaces facing into the flow. Molecules reflect diffusively from the surface with translational and internal energies sampled at the surface temperature. Effects of lower accommodation coefficients will also be assessed.

Flow Boundary Conditions

In simulating highly rarefied flows, the computational flow domain must extend far enough upstream of the body to provide ample opportunity for freestream molecules to interact with those molecules that have reflected from the body and are diffusing into the flow. Insufficient upstream domain size leads to overprediction of aerodynamic heating and forces.^{2,13}

Taking advantage of body symmetry, the simulated flowfield configuration is that of a wind tunnel depicted for pitch simulations in Fig. 4 (100L x 84H x 18W in cells) with a specularly reflecting symmetry plane and a free-molecular outer plane. Particles that strike the outer plane after reflecting off a body surface are removed from the flowfield. All other particles striking the outer plane reflect specularly back into the flow. This effectively reduces the influence that the outer wall has upon the flow near the vehicle in highly rarefied or free-molecular flows.

Particles enter the flow domain from the left plane at the specified pitch angle, and may exit from the right plane. The top and bottom planes represent free-molecular periodic boundary conditions. Again, particles that had reflected from the body before striking these planes are removed from the simulation. All other particles striking one of these planes simply re-enter the flow domain from the opposite plane, maintaining their velocity vectors. This boundary condition still provides freestream flow approaching the body geometry while reducing the required height of the wind tunnel, therefore minimizing the size and cost of the simulation.

Simulation Results

Employing a freestream flow speed of $u_\infty = 8.6$ km/s and the day-side atmospheric data of Keating,¹⁴ simulations were performed for several entry attitudes of pitch, yaw, and solar-panel canting. Flight conditions are listed in Table 1 for each altitude. Results from the particle simulation for rarefied flows, employing the finite molecular mean free path, were compared to free-

Table 1 Simulation flowfield specifications

Altitude, km	ρ_∞ , kg/m ³	T_∞ , K	m , g/mole	M_∞	Kn_∞^a
136	1.39×10^{-8}	217	40.1	35.2	2.819
138	9.24×10^{-9}	222	39.4	34.6	4.222
140	6.13×10^{-9}	225	38.9	34.0	6.324

^aBased on HGA diameter of 370 cm, $Kn_\infty = \lambda_\infty/D$.

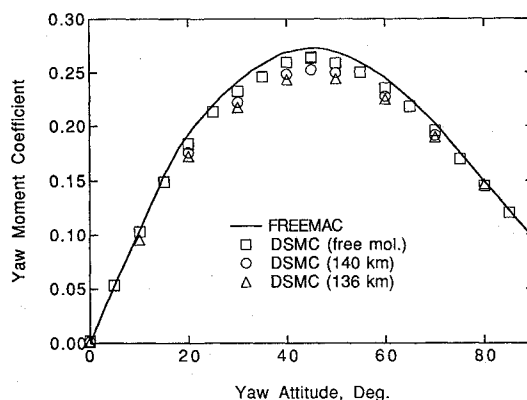


Fig. 5 Coefficient of restoring yaw moment vs entry yaw attitude.

molecule (collisionless flow) simulation results. Both of these were, in turn, compared to analytic free-molecule results generated with the FREEMAC code,³ which employs ray-tracing algorithms to assess aerodynamic coefficients of spacecraft. FREEMAC results employed the exact same vehicle geometry as used in the DSMC solutions, but assumed that all surfaces have a fixed temperature of 300 K. The DSMC code predicted surface temperatures near 400 K for the solar panels using the radiative equilibrium model described above.

Limited computational resources and the large number of cases investigated in the present study restricted the number of particles that could be employed in the simulation to just four particles per cell in the freestream. However, density gradients in the flowfield significantly increased the particle densities near body surfaces so that 400,000 particles existed typically in the flowfield at steady state. Employing roughly 6000 transient steps and 6000 steady-state sampling steps in the simulation, the number of statistical samples was sufficiently large to yield accurate and meaningful solutions. Run times averaged 1.0–2.0 CPU hours per case on the Cray-YMP supercomputer with a nominal computational performance of roughly 1.1 μ s per particle per timestep. The simulation could have employed 10 times as many particles but would have required a 10-fold increase in computational time per case, which was not warranted in the present study.

The simulation computed the net force and heat flux upon each surface facet of the vehicle. Torques were computed by the moments of body forces about a reference point defined by the intersection of the central body axis (x axis) and the solar-panel axis (y axis). This reference point is very close to the spacecraft center of mass. Coefficients for forces and moments are defined from freestream velocity and density, the simulated frontal area, and a reference length for moments given by the HGA diameter.

Pitch and Yaw Aerodynamics

Moment coefficients for yaw and pitch attitudes (0–90 deg) are plotted in Figs. 5 and 6 as computed with the FREEMAC and DSMC codes. The thermal accommodation coefficient was fixed at unity for both codes. For all cases, the resulting moments acted to return the vehicle to its nominal zero-pitch, zero-yaw attitude. Yaw moments rose smoothly, reaching a peak at roughly 45 deg before dropping again. The pitching moment, however, had two local maxima (at 20 and 70 deg) and a local minimum (at 50 deg). This behavior resulted from the solar panels shading the HGA partially from the incident flow at those attitudes.

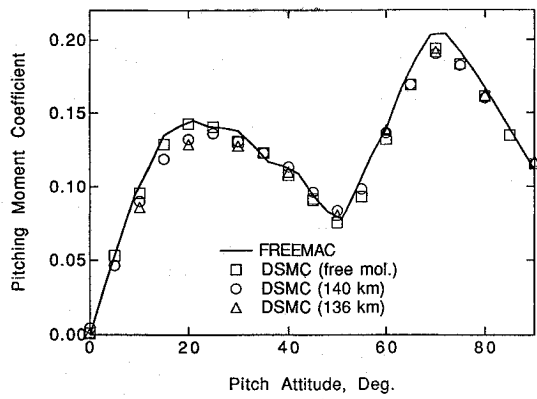


Fig. 6 Coefficient of restoring pitching moment vs entry pitch attitude.

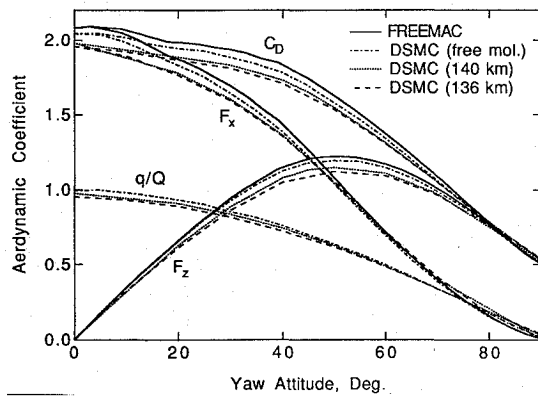


Fig. 7 Aerodynamic coefficients vs yaw attitude.

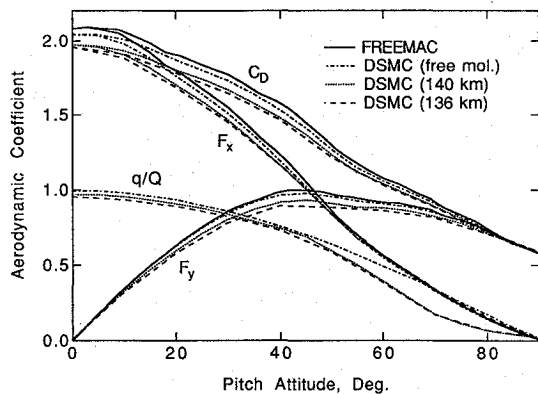


Fig. 8 Aerodynamic coefficients vs pitch attitude.

The DSMC method was used to simulate rarefied flows (finite mean free path) at 136 and 140 km. Repeating these simulations under free-molecular conditions yielded results that were nearly indistinguishable between the two altitudes. Note that the DSMC free-molecular results agree fairly well with those from FREEMAC. Slight differences are likely due to different surface-temperature models employed in each code and the fact that FREEMAC neglects multiple reflections of molecules with vehicle surfaces. More important, however, is the observation that the rarefied and free-molecular DSMC results do not differ dramatically, indicating that molecular collisions do not alter the vehicle aerodynamics significantly. The moments for rarefied flow at 136 km are roughly 7–10% below the free-molecular results, except at high pitch and yaw attitudes. The results are similar at 140 km.

Other aerodynamic properties under yaw and pitch are plotted in Figs. 7 and 8. These include force coefficients in the direction of the body axis (F_x), in the perpendicular directions (F_y and F_z), and in the flow direction (drag, C_D). The net heat flux on the windward solar panel is plotted relative to the incident freestream energy flux.

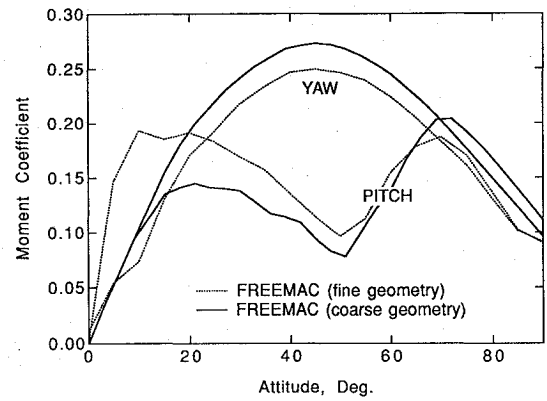


Fig. 9 Effect of FREEMAC body resolution on predicted moment coefficients.

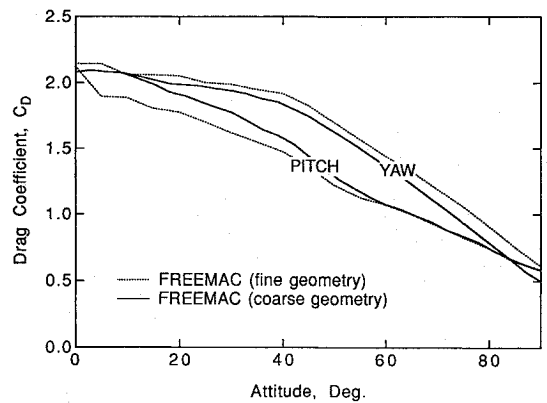


Fig. 10 Effect of FREEMAC body resolution on predicted drag.

For all coefficients, the effects of flow rarefaction led to small yet noticeable differences from free-molecular results. These differences are greatest at lower pitch and yaw attitudes, where the solar panels and HGA led to greater wetted area of the vehicle. At attitudes near 90 deg, the wetted area was significantly smaller, so that the flow was effectively more rarefied, leading to little distinction between rarefied and free-molecular results.

Effect of Body Resolution

The FREEMAC and DSMC results above employed identical vehicle geometries defined at a rather coarse body resolution. This was sufficient to demonstrate the small differences between rarefied and free-molecular flow models. However, the FREEMAC code may employ a fine body resolution that more precisely resembles the actual vehicle configuration, including small features such as the MGA, LGA, ALTA, and REM. These small features would not alter the effects of flow rarefaction demonstrated above, but they do affect the magnitudes of vehicle aerodynamics. Moment and drag coefficients for each body resolution are plotted in Figs. 9 and 10 as computed with the FREEMAC code only. Note that the same general pitch and yaw characteristics result for each body resolution, but that the magnitudes differ somewhat. Accurate estimation of the vehicle aerodynamics would therefore require adjusting the fine-resolution FREEMAC results to account for the small rarefaction effects demonstrated with the coarse resolution above.

"Windmill" Roll Aerodynamics

A creative experiment suggested by Lyons and Hurlbut¹⁵ for Magellan aerobraking would involve canting the solar panels in opposite directions to create a "windmill" configuration with the spacecraft. Measuring the restoring roll torques induced by the spacecraft control system would provide insight into rarefied hypersonic gas-surface interaction. This windmill configuration was simulated with the DSMC code in the present work for flow in the nominal direction (along the body axis) at 138-km altitude. The

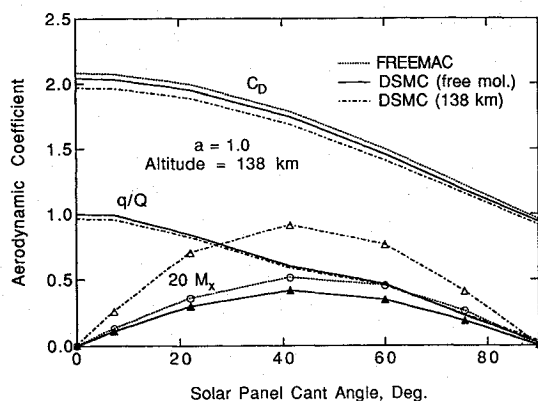


Fig. 11 Aerodynamic coefficients vs solar-panel cant angle.

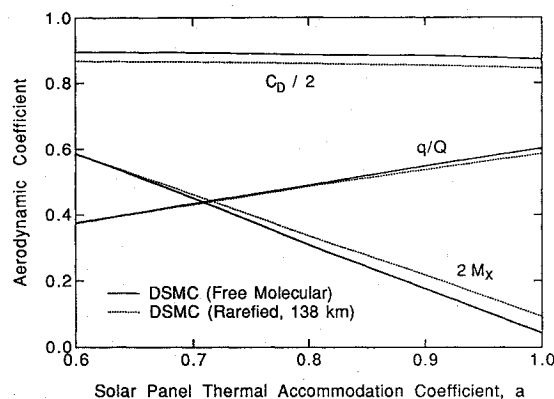


Fig. 12 Aerodynamic coefficients vs thermal accommodation coefficient a .

solar panels were canted at angles of 0, 7.2, 22.0, 41.4, 60, 75.5, and 90 deg, where 0 deg is perpendicular to the incident flow. The thermal accommodation coefficient was fixed at unity. Coefficients for drag, roll moment, and panel heating are plotted in Fig. 11. Drag and heating results exhibit the same differences between rarefied and free-molecular flows as predicted above from the pitch and yaw simulations. However, the roll moment coefficients in the rarefied simulations were nearly twice as large as those in the free-molecular flows. Although these roll moments are very small, and therefore statistically sensitive, they exhibit this behavior consistently for all cant angles.

This surprising behavior is unlike all other aerodynamic observations in this study, leading to concern about the solution's validity. It was suggested that perhaps the DSMC flow domain was so small that particles diffusing out of the periodic simulation boundaries were reflecting back toward the body, thus altering the roll characteristics of the vehicle. The simulations were repeated three times with consecutively larger lateral domains (in the y and z directions). The distance between the vehicle surfaces and the nearest boundary was increased by factors of 3, 6, and 20. Nonetheless, the roll moment coefficients for each case differed from the original by less than 5%. These results indicate that, indeed, the roll moment for the windmill configuration is small but highly sensitive to molecular collisions in the rarefied flowfield.

Effects of Surface Accommodation

In the DSMC code, a thermal accommodation coefficient of, say, $a = 0.8$ means that particles have a 20% chance of reflecting specularly from a surface and an 80% chance of reflecting diffusely with energies sampled at the surface temperature. Windmill roll-moment calculations with panels canted at 41.4 deg were repeated using thermal accommodation coefficients of $a = 0.6, 0.7, 0.8$, and 0.9 . Results for free-molecular and rarefied flows are plotted in Fig. 12. With increasing thermal accommodation coefficient, the roll moment dropped rapidly while panel heating increased. More importantly, the difference between rarefied and free-molecular results was significant only for coefficients above $a = 0.80$.

Shortly after all of the present calculations were completed, limited flight data from the nominal aeropasses in 1993 became available and indicated that heating of the solar panels was 20–30% below that computed when assuming free-molecule conditions and $a = 1$ in the FREEMAC and DSMC codes. Effects of molecular collisions in the flow account for roughly 7% of that difference²; the remaining energy deficit was likely due to the inaccuracy of the assumed accommodation coefficient. Rather than $a = 1$ as used in the calculations, the flight data suggest that coefficients in the range $a = 0.75$ – 0.85 would be more appropriate. Gas-surface interaction is one of the least understood, yet admittedly most important, aspects of simulating rarefied gasdynamics for entry craft. These observations further support the assertion that the windmill experiment would provide valuable flight data regarding surface accommodation and flowfield properties under flight conditions.

Concluding Remarks

At free-molecule conditions, the FREEMAC code is a most appropriate tool for simulating the aerodynamics of the Magellan spacecraft during proposed entry into the atmosphere of Venus. However, at nominal altitudes near 140 km, where the freestream Knudsen number drops below $Kn = 10$, the free-molecular flow assumption itself could be questionable. This study computed the body torques on the spacecraft, when entering with various off-design attitudes, using a DSMC particle method for rarefied flow conditions. Repeating these simulations for collisionless flow provided a direct means of assessing the significance of molecular interactions in the flow, as well as providing a means to validate the technique through comparison with FREEMAC results. At all pitch and yaw attitudes, molecular collisions tended to reduce the aerodynamic forces, moments, and heating below free-molecular values by 7–10%. All body torques acted to restore the vehicle to its nominal zero-pitch, zero-yaw attitude. Canting of the solar panels yielded roll moments that were highly sensitive to the thermal accommodation coefficient for gas-surface interaction. For coefficients near unity, the predicted roll moments were notably larger for rarefied flows than for free-molecular flows. Uncertainty in the accommodation coefficient limits the accuracy of predicted aerodynamics by any simulation method in the near-free-molecule regime. However, the present study conclusively demonstrates that molecular collisions lead to small, yet noticeable differences from free-molecular predictions at the flight conditions for Magellan aerobraking.

Acknowledgments

The authors gratefully acknowledge the assistance and technical support of Daniel Lyons (JPL), and the support of NASA Ames Research Center and Martin Marietta Astronautics Company in the use of their facilities. This work was sponsored in part (for B.L.H.) by NASA Grant NCC 2-582 to Eloret Institute.

References

- Lyons, D. T., Sjogren, W., Johnson, W. T. K., Schmitt, D., and McDonald, A., "Aerobraking Magellan," American Astronomical Society, Paper 91-420, Aug. 1991.
- Haas, B. L., and Feiereisen, W. J., "Particle Simulation of Rarefied Aeropass Maneuvers of the Magellan Spacecraft," AIAA Paper 92-2923, July 1992; also *Journal of Spacecraft and Rockets* (to be published).
- Fredo, R. M., and Kaplan, M. H., "Procedure for Obtaining Aerodynamic Properties of Spacecraft and Rockets," *Journal of Spacecraft and Rockets*, Vol. 18, No. 4, 1981, pp. 367–373.
- Rault, D. F. G., "Aerodynamic Characteristics of the Magellan Spacecraft in the Venus Upper Atmosphere," *Journal of Spacecraft and Rockets*, Vol. 31, No. 4, 1994, pp. 537–542.
- Bird, G. A., *Molecular Gas Dynamics*, Clarendon, Oxford, England, UK, 1976.
- Baganoff, D., and McDonald, J. D., "A Collision-Selection Rule for a Particle Simulation Method Suited to Vector Computers," *Physics of Fluids A*, Vol. 2, July 1990, pp. 1248–1259.
- McDonald, J. D., "A Computationally Efficient Particle Simulation Method Suited to Vector Computer Architectures," Ph.D. Thesis, Stanford Univ., Stanford, CA, Dec. 1989.

⁸Bird, G. A., "Monte-Carlo Simulation in an Engineering Context," *Rarefied Gas Dynamics*, edited by S. S. Fischer, Part I, AIAA, New York, 1981, p. 239.

⁹Borgnakke, C., and Larsen, P. S., "Statistical Collision Model for Monte Carlo Simulation of Polyatomic Gas Mixture," *Journal of Computational Physics*, Vol. 18, No. 4, 1975, p. 405.

¹⁰Bird, G. A., "Definition of Mean Free Path for Real Gases," *Physics of Fluids*, Vol. 26, No. 11, 1983, pp. 3222-3223.

¹¹Haas, B. L., "Particle Simulation of Satellite Aerobraking with Coupled Surface Heat Transfer," *Rarefied Gas Dynamics: Space Science and Engineering*, edited by B. D. Shizgal and D. P. Weaver, Vol. 160, Progress in Astronautics and Aeronautics, AIAA, Washington, DC, 1994, pp. 44-52.

¹²Haas, B. L., "Models for Dynamic Surface Temperatures during Rarefied Aeropass Maneuvers," AIAA Paper 93-2765, July 1993.

¹³Haas, B. L., Fallavollita, M. A., "Flow Resolution and Domain Influence in Rarefied Hypersonic Blunt-Body Flows," *Journal of Thermophysics and Heat Transfer*, Vol. 8, No. 4, 1994, pp. 751-757.

¹⁴Kliore, A. J., Moroz, V. I., and Keating, G. M., *Venus International Reference Atmosphere*, Vol. 5, 1986, pp. 142-148.

¹⁵Lyons, D. T., and Hurlbut, F. C., "Measuring the Lift coefficient in Free Molecular Flow while Aerobraking Magellan," *Rarefied Gas Dynamics: Space Science and Engineering*, edited by B. D. Shizgal and D. P. Weaver, Vol. 160, Progress in Astronautics and Aeronautics, AIAA, Washington, DC, 1994, pp. 53-63.